

# Probing Liquid–Liquid Interfaces with Spatially Resolved NMR Spectroscopy

Jörg Lambert, Roland Hergenröder, Dieter Suter, and Volker Deckert\*

Phenomena occurring at the interface between two immiscible liquids have a deep impact on many processes of everyday life.<sup>[1]</sup> The stability of emulsions depends on the interaction of proteins or surfactants at the oil–water interface.<sup>[2]</sup> Solvent extraction and phase-transfer catalysis rely on optimizing reactions at the boundary of two liquids. Moreover, the liquid–liquid interface between an organic solvent and water represents a simple model of a biological membrane. Historically, the knowledge of the structure<sup>[3]</sup> and dynamics<sup>[4]</sup> of liquid–liquid interfaces mainly stemmed from surface-tension measurements and thermodynamic analysis.<sup>[1]</sup> Over the last couple of decades probing of liquid–liquid interfaces using nonlinear optical methods has developed.<sup>[5]</sup> Many traditional bulk techniques have been adapted for studying the interface. Second-harmonic generation and vibrational sum-frequency (VSF) spectroscopy both provide information that is inherently surface-specific.<sup>[6]</sup> The latter, coupled with molecular dynamics,<sup>[7]</sup> helped to unravel the structure of many interfaces. X-ray<sup>[8]</sup> and neutron<sup>[9]</sup> scattering have also been applied to study liquid–liquid interfaces and can provide useful and reliable information on the interfacial widths formed. Surface second-harmonic generation mainly uses molecular probes (such as push–pull molecules) to evaluate surface effects.

Probing liquid–liquid interfaces with scanning probe techniques still remains a challenge, though first results from atomic force microscopy (AFM)<sup>[10]</sup> and scanning electron microscopy (SEM)<sup>[11]</sup> have been obtained. Transient phase grating experiments with evanescent fields resulting from total internal reflection at an interface between a polar absorbing and a nonpolar transparent phase were used to measure the dimension of liquid–liquid interfaces.<sup>[12]</sup> Vibrational sum frequency spectroscopy (VSF)<sup>[13]</sup> selectively probes the molecular structure at hydrocarbon–water interfaces and shows that the hydrogen bonding between adjacent water molecules at the interface is weak and results in a

substantial orientation of the water molecules in the interfacial region.<sup>[14]</sup> Scanning electrochemical microscopy (SECM) can be used to study localized processes occurring at liquid–liquid interfaces.<sup>[15]</sup>

In general, investigations of liquid–liquid interfaces impose a significant technical challenge: the discrimination between the information contained in the miniscule volume of the interface and that from the abundant bulk liquid. Apart from the above-mentioned nonlinear optical techniques, only one approach exists to obtain structural information without modifying the interface. The combination of near-field microscopy and Raman spectroscopy<sup>[16,17]</sup> in order to obtain information of gradual changes correlated with distance towards the interface has been also presented. Illumination of a sample surface with a near-field probe provides high spatial resolution beyond the diffraction limit, and theoretically the depth resolution for a 100 nm aperture lies at approximately 10 nm. In combination with Raman spectroscopy this results in highly resolved information on the molecular structure of the surface. The drawback of the technique is the use of a probe that must be very close to the surface. As soon as the interface contacts the tip, a meniscus is formed and the entire experiment must be restarted. In addition this probe can already influence the results by adding a further component into the system.

Here, we present a technique based on volume-selective nuclear magnetic resonance (NMR) spectroscopy,<sup>[18]</sup> which induces no mechanical perturbation of the interface while also providing a high chemical contrast. Volume-selective NMR spectroscopy restricts the detection of magnetic resonance data to a detection volume element of definable size and position. This mode is well known, for instance, from medical applications. The volume of the voxel (a volume element that represents a property on a regular grid in three-dimensional space) is determined by the desired spatial resolution as well as by the required detection limit and sensitivity of the NMR experiment. The crucial point is to use a cuboid voxel geometry with a small width in the direction orthogonal to the interface of interest and larger dimensions elsewhere: in obtaining information on a liquid–liquid interface, not all three spatial dimensions are equally important. Fluctuations parallel to the interfacial surface will be slow on NMR timescales and hence can be neglected.

The voxel geometry used in our experiments is shown schematically in Figure 1. Basically the number of spins required for the NMR signal is achieved by extending the voxel size parallel to the surface while at the same time reducing the size orthogonal to the surface. Thus in this voxel geometry the number of spins contributing to a signal is the same as that for a cubic voxel. The resolution in the dimension

[\*] Priv.-Doz. Dr. V. Deckert

Department of Proteomics, ISAS—Institute for Analytical Sciences  
Bunsen-Kirchhoff-Strasse 11, 44139 Dortmund (Germany)

and

IPHT – Institut für Photonische Technologien

Albert-Einstein-Straße 9, 07745 Jena (Deutschland)

Fax: (+49)3641-206-139

E-mail: volker.deckert@ipht-jena.de

Homepage: <http://www.ipht-jena.de>

Dr. J. Lambert, Dr. R. Hergenröder

Department of Material Analysis, ISAS, Dortmund (Germany)

Prof. Dr. D. Suter

Lehrstuhl Experimentelle Physik 3

Technische Universität Dortmund (Germany)

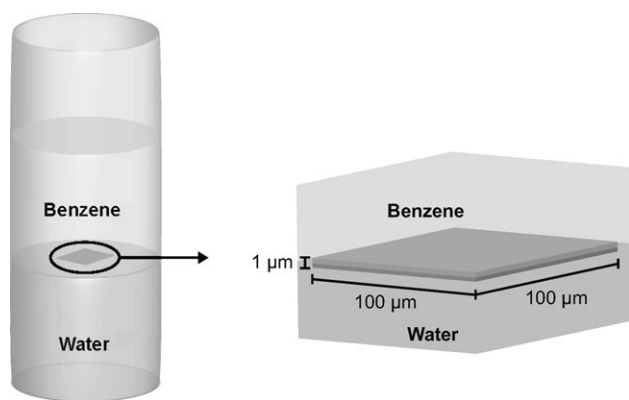


**Figure 1.** The voxel used for spatial selection has a cuboid shape, which assures sufficient resolution in the direction of interest as well as sufficient spins for a good signal-to-noise ratio.

of interest is improved by sacrificing resolution in the other two dimensions of less importance.

The detection voxel can be shifted within the liquid sample to any position by changing the carrier frequency of one of the selective NMR pulses, that is, without the use of any mechanical equipment interfering with the sample or generating vibrations. By approaching the interface in (sub-)micrometer steps starting from one of the bulk phases, structural and compositional changes can be detected from the measurement of the chemical shifts and signal intensities, respectively. Figure 2 shows a pseudo three-dimensional representation and an image plot of a series of  $^1\text{H}$  NMR spectra as obtained with the volume-selective NMR technique for the system water–benzene.

A volume element of the size  $250 \times 250 \times 1 \mu\text{m}^3$  is shifted in steps of 50 nm from the bulk benzene phase across the

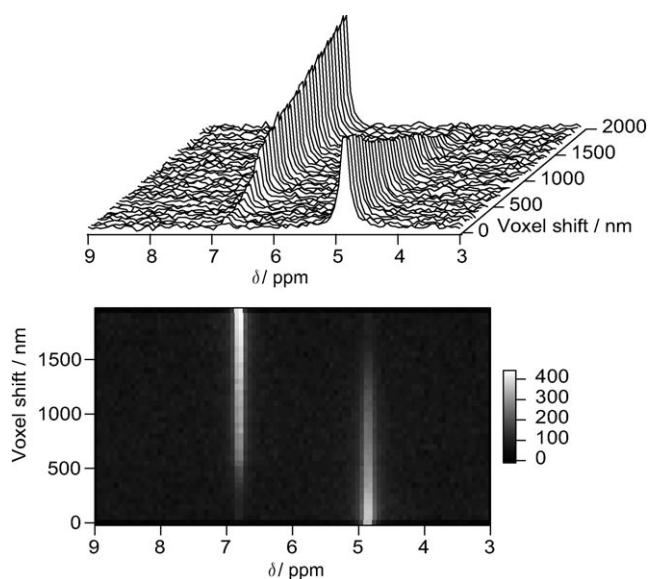


**Figure 2.** A series of volume-selective  $^1\text{H}$  NMR spectra recorded for the system benzene–water in a pseudo three-dimensional representation as well as an image plot. For details see the text and the Experimental Section.

interface into the water phase. In the present experiment approximately twenty subsequent traces contain signals of both benzene and water, which is well in agreement with a detection volume thickness of  $1 \mu\text{m}$  and the shift increment of 50 nm, both measured orthogonal to the liquid–liquid interface. The thickness of the water–benzene interface for the applied detection dimensions can be safely neglected. The voxel dimensions are limited by the present setup in terms of the strength of the field gradient in the  $z$  direction,  $G_z = 1 \text{ T m}^{-1}$ . In principle, however, field gradients of  $100 \text{ T m}^{-1}$  corresponding to resolutions down to 10 nm can be achieved. Possible limitations of the spatial resolution, such as disturbances at the water–benzene interface (surface tension:  $35 \text{ mN m}^{-1}$ ) by thermally excited capillary waves, are of the order of a few nm and are far below the length scale of the measurements.<sup>[19]</sup>

The impact of diffusion on the limitation of the spatial resolution is usually overestimated. Under conditions of free translational diffusion a mean free path  $\langle x^2 \rangle = 2Dt_{\text{seq}}$  (where  $t_{\text{seq}}$  is the duration of the pulse sequence) of  $10 \mu\text{m}$  is calculated, assuming a typical diffusion coefficient  $D = 10^{-9} \text{ m}^2 \text{ s}^{-1}$  and  $t_{\text{seq}} = 60 \text{ ms}$ . Molecular dynamics studies, however, suggest, that the self-diffusion near liquid–liquid interfaces is anisotropic. If the self-diffusion is described by diffusion coefficients tangential ( $D_{s,T}$ ) and normal ( $D_{s,N}$ ) to the interfacial plane, theoretically it is predicted that  $D_{s,T} > D_{s,N}$  near the interface.<sup>[20]</sup> However, in the bulk the diffusion is isotropic. To get experimental evidence, we performed NMR gradient echo diffusion measurements<sup>[21]</sup> on the benzene–water system studied here. An excitation sequence employing a selective RF pulse in the presence of a  $G_z$  gradient was used to select a slice of  $10 \mu\text{m}$  comprising the benzene–water interface. For benzene and water, a reduction of  $D_{s,N}$  by a factor of 5.4 and 4.8, respectively, was found relative to  $D_{s,T}$ . The roughly fivefold reduction of  $D_{s,N}$  for benzene and water a few micrometers from the surface relative to the bulk value weakens the diffusion limitation usually claimed for volume-selective NMR experiments and helps to enhance the spatial resolution by one order of magnitude into the micrometer range. As an explanation for this, it is assumed that the occurrence of a translational barrier impermeable for the translating spins results in the reduction of the translational mean free path perpendicular to the surface.<sup>[20]</sup> Higher spatial resolution in the nanometer range can be established following two strategies: both extension of the selective pulse for the  $z$  direction and the application of larger  $z$ -gradient strengths allow smaller slices to be excited. While the former strategy prolongs the sequence duration  $t_{\text{seq}}$  interfering even with the “weakened” translational diffusion limitation, the latter strategy keeps the sequence duration constant and is clearly the method of choice.

In conclusion, we have demonstrated a novel approach for the investigation of liquid–liquid interfaces at high spatial resolution. The key issue is the use of a flat cuboid as the detection volume element. This shape preserves a sufficient number of spins that contribute to the NMR signal while maintaining high spatial resolution in the direction of interest. We found that the diffusion coefficient at the interface is five times smaller than that in the bulk. As a result measurements

with increased resolution in the low nanometer range should be feasible and potentially allow the observation of molecular changes at the interface. Future investigations comprise studies of surfactants at the interface in order to model biomembranes, as well as the improvement of the spatial resolution perpendicular to the surface by the application of higher gradient strengths.

### Experimental Section

Measurements were performed at a field strength of 14.1 T (600 MHz) in a 15 mm sample tube in order to reduce the effects of the capillary curvature on the interface. Doubly distilled water and analytical-grade benzene were used to prepare the sample. The STEAM<sup>[18]</sup> technique was used for volume selection. The size of the detection volume element was chosen  $250 \times 250 \times 1 \mu\text{m}^3$  in the  $x$ ,  $y$ , and  $z$  direction, with the  $z$  direction being orthogonal to the liquid–liquid interface. The extended dimensions in the  $x$  and  $y$  direction were selected for sensitivity reasons. Subsequent, overlapping slices in the  $z$  direction are 50 nm apart, corresponding to a carrier frequency increment of 2.15 Hz. Gradient strengths in the  $x$ ,  $y$ , and  $z$  direction were  $G_x = 95.8 \text{ mT m}^{-1}$ ,  $G_y = 96.9 \text{ mT m}^{-1}$ , and  $G_z = 1010 \text{ mT m}^{-1}$ , respectively. Bandwidths of the selective  $90^\circ$  pulses in the  $x$ ,  $y$ , and  $z$  direction were 1.03 kHz, 1.02 kHz, and 43 Hz, respectively. 112 scans were recorded for each increment. For the diffusion measurements, a selective sinc-shaped  $90^\circ$  pulse of bandwidth 100 Hz and a field gradient of  $G_z = 234 \text{ mT m}^{-1}$  were used for excitation.

Received: March 12, 2009

Published online: July 13, 2009

**Keywords:** liquid–liquid interfaces · NMR spectroscopy · spatially resolved NMR spectroscopy

- [1] I. Benjamin, *Annu. Rev. Phys. Chem.* **1997**, *48*, 407–451.
- [2] S. Tamilvanan, *Prog. Lipid Res.* **2004**, *43*, 489–533.
- [3] J. Chowdhary, B. M. Ladanyi, *J. Phys. Chem. B* **2006**, *110*, 15442–15453.
- [4] S. Tsukahara, *Anal. Chim. Acta* **2006**, *556*, 16–25.
- [5] A. G. Lambert, P. B. Davies, D. J. Neivandt, *Appl. Spectrosc. Rev.* **2005**, *40*, 103–145.
- [6] X. Y. Chen, M. L. Clarke, J. Wang, *Int. J. Mod. Phys. B* **2005**, *19*, 691–713.
- [7] J. B. Buhn, P. A. Bopp, M. J. Hampe, *J. Mol. Liq.* **2006**, *125*, 187–196.
- [8] M. L. Schlossman, *Phys. B* **2005**, *357*, 98–105.
- [9] A. Zarbakhsh, A. Querol, J. Bowers, *Langmuir* **2005**, *21*, 11704–11709.
- [10] D. Filip, V. I. Uricanu, M. H. G. Duits, *Langmuir* **2005**, *21*, 115–126.
- [11] K. Adachi, K. Chayama, H. Watarai, *Chirality* **2006**, *18*, 599–608.
- [12] P. Brodard, E. Vauthey, *J. Phys. Chem. B* **2005**, *109*, 4668–4678.
- [13] L. F. Scatena, M. G. Brown, G. L. Richmond, *Science* **2001**, *292*, 908–912.
- [14] G. L. Richmond, *Chem. Rev.* **2002**, *102*, 2693–2724.
- [15] G. Wittstock, M. Burchardt, S. E. Pust, Y. Shen, C. Zhao, *Angew. Chem.* **2007**, *119*, 1604–1640; *Angew. Chem. Int. Ed.* **2007**, *46*, 1584–1617.
- [16] M. De Serio, H. Mohapatra, R. Zenobi, V. Deckert, *Chem. Phys. Lett.* **2006**, *417*, 452–456.
- [17] M. De Serio, A. N. Bader, M. Heule, R. Zenobi, V. Deckert, *Chem. Phys. Lett.* **2003**, *380*, 47–53.
- [18] S. F. Keevil, *Phys. Med. Biol.* **2006**, *51*, R579–R636.
- [19] J. Jäckle, *J. Phys. Condens. Matter* **1998**, *10*, 7121–7131.
- [20] D. S. Grebenkov, *Rev. Mod. Phys.* **2007**, *79*, 1077–1137.
- [21] B. Stejskal, J. Tanner, *J. Chem. Phys.* **1965**, *42*, 288.